*J. Phycol.* **56,** 1676–1686 (2020)

DOI: 10.1111/jpy.13054

# STRUCTURAL VARIATIONS INCREASE THE UPPER LIMIT OF COLONY SIZE OF *MICROCYSTIS*: IMPLICATIONS FROM LABORATORY CULTURES AND FIELD INVESTIGATIONS[1]

*Ganyu Feng*, *Wei Zhu*[2]

College of Environment, Hohai University, Nanjing, Jiangsu 210098, China

*Zongpu Xue*

College of Hydrology and Water Resources, Hohai University, Nanjing, Jiangsu 210098, China

*Siyuan Hu*

Key Laboratory of Integrated Regulation and Resource Development on Shallow Lakes, Ministry of Education, College of Environment, Hohai University, Nanjing, Jiangsu 210098, China

*Ruochen Wang, Shuai Zhao, and Huaimin Chen*

College of Environment, Hohai University, Nanjing, Jiangsu 210098, China

**Wild *Microcystis* have highly diverse colonial structures and sizes, including variable colony geometry, cell arrangement, and diameter. These structural and dimensional variations may play an important role in continual, frequent *Microcystis* blooms during summer and autumn, the cause of which still remains unclear. Here, laboratory cultures and field investigations were applied to assess mechanisms that drive variation in structure and size, as well as factors that influence diversity. The results demonstrated that colonies grew to large sizes at the expense of their structure being loose and inhomogeneous. Furthermore, colonies may spontaneously change structure to relieve the constraints of size in return. Influencing factors (nutrient limits and turbulent shear) tended to promote these variations. Our work highlights that the diversity of *Microcystis* colonies may be a result of structural variations as survival strategies for gaining a higher upper size limit. Therefore, during seasonal successions, large colonies commonly have porous or loosely arranged structures, such as in *M. aeruginosa*. Additionally, this study hypothesized three possible transition routes for better understanding structural diversity and variations in *Microcystis*.**

***Key index words: Microcystis*; colony; structural variation; size limit; morphology strategies**

***Abbreviations*: *B*, thickness of colony; $B_{Max}$, maximum thickness; *c*, tightness; $c_c$, peripheral tightness; $c_c^i$, peripheral tightness of a prism; *CDR*, cell distribution ratio; $c_r$, internal tightness; $c_{sur.}$, cell number per surface area of a colony; $c_{sur.}^i$, cell number per top face area of a prism; $c_0$, cell concentration in water; *D*, colony diameter; DTP, total dissolved phosphorus; DTN, total dissolved nitrogen; $D_{50}$, median diameter; *H*, microscope objective distance; H-Type, homogeneous type; *i*, serial number of prisms; IMR, interval maxima regression; *Lab-s*, colonies from motionless culture conditions; *Lab-t*, colonies from oscillatory culture conditions; L-Type, looser-periphery type; $NH_4^+$-N, ammonia nitrogen; $N_S^{i\prime}$, cell number in the top face of a prism; OR, linear regression analysis of all data; *S*, area of colony; $S_i'$, top face area of a prism; TP, total phosphorus; TN, total nitrogen; T-Type, tighter-periphery type; *V*, colony volume**

Cyanobacteria blooms are hazardous to humans (Jochimsen et al. 1998, Paerl and Otten 2013), of which *Microcystis* blooms occur frequently in hypertrophic and eutrophic waters, such as the Taihu, Dianchi, and Chaohu lakes of China (Qin et al. 2019, Shan et al. 2019, Su et al. 2019). There are many ways to forecast the dynamics of *Microcystis* blooms (Verspagen et al. 2014, Aparicio Medrano et al. 2016). However, long-term forecasting still poses challenges. There is a mismatch between biomass measured in the field and what is predicted in the laboratory (Xiao et al. 2020). One of the reasons is because the colonial structure and size dynamics of *Microcystis* are still difficult to simulate.

In laboratory cultures, *Microcystis* are commonly single cells (Xiao et al. 2018); however, they can maintain colonies in the wild (Reynolds et al. 1981). In the wild, colony size increases from spring to autumn and decreases when the weather turns cold. During summer and autumn, when blooms are most frequent, loosely arranged *M. wesenbergii* and

[1]Received 7 April 2020. Accepted 6 July 2020.
[2]Author for correspondence: e-mail: zhuweiteam.hhu@gmail.com.
Editorial Responsibility: T. Mock (Associate Editor)

perforated *M. aeruginosa* are dominant morphospecies. During winter and early spring, common *Microcystis* include small-sized *M. ichthyoblabe* with $D_{50} < 100$ μm (Zhu et al. 2018). $D_{50}$ is the median diameter of colonies, whereby 50% of the total volume of particles is smaller than this diameter. *Microcystis ichthyoblabe* colonies are small with a $D_{50}$ limit of 300–400 μm; however, *M. aeruginosa* and *M. wesenbergii* are much larger with $D_{50}$ values of 400–700 μm (Li et al. 2013a). Therefore, the morphology and dimension of colonies are seasonally diverse, which probably benefits *Microcystis* in being dominant during bloom formation.

There is strong evidence that large colony size facilitates the formation of surface blooms (Reynolds et al. 1981, Gan et al. 2012). The greatest benefit of increasing colony size is the ability to float more easily (Wu and Kong 2009, Yamamoto et al. 2011), enhancing its ability to reach the water surface and receiving more light than other phytoplankton (Kromkamp and Walsby 1990). Colony formation also protects against environmental stresses or threats, such as zooplankton and poisonous substances (Yang et al. 2009, Shen et al. 2011, Wu et al. 2018). Therefore, *Microcystis* has developed a sound ecological strategy with a series of adaptation characteristics through colony formation. In addition, stressful influencing factors or threats also cause colony's maintenance (Xiao et al. 2018), such as turbulent shear and nutrient levels (Duan et al. 2018, Li et al. 2018). The functional degradation of *Microcystis*, where there is a loss of wild-type morphologies during laboratory cultivations, might be a result of relatively suitable growing conditions.

Comprehensive data show that a large size is disadvantageous for the growth of photosynthetic organisms, especially the energy metabolism and nutrient quality of intra-colony cells (Nielsen et al. 1996). *Microcystis* colonies were found to have a growth rate of $0.2–0.4 \cdot d^{-1}$, which was lower than that of single cells (Li et al. 2013b) and negatively related to the size of colonies (Wilson et al., 2010). Additionally, inorganic carbon, light intensity, and dissolved oxygen were reported non-uniformly distributed or internally restricted in large colonies (Paerl 1983, Fang et al. 2018, Feng et al. 2019). These findings raise the question of how the structures of colonies respond to elevated colony size and concomitant intra-colony resource limits. The results may enable better understanding the ecological benefits of structural variations in *Microcystis*.

Due to the seasonal diversity in colony morphology and dimension as described above, this study supposes that stress or pressure can force or induce *Microcystis* to alter its structure and size. A recent investigation demonstrated a tradeoff between colony size and structure, whereby large colonies tended to grow loosely in order to relieve intra-colony light limitations (Feng et al. 2019). The theory indicated the potential formation of holes or pores in large colonies, which might be a transitional stage between *M. ichthyoblabe* and *M. aeruginosa*, and was analyzed in the present study. This study aimed to gain new insight into the colonial structure as well as its relation to colony size and influential factors. Here, the colonial structure was characterized as shape and cell arrangement of colonies; size was characterized as diameter and thickness of colonies. The heterogeneity of cell arrangement was estimated by the cell distribution ratio (*CDR*; i.e., the ratio of peripheral tightness to internal tightness). Turbulent shear and nutrient limits were considered in laboratory cultures.

## MATERIALS AND METHODS

*Colonial structure and colony size analysis.* To investigate the size and structure of *Microcystis* colonies, this study analyzed their diameter, thickness, shape, and cells arrangement. Perforated colonies were regarded as *M. aeruginosa*; homogeneous, spherical colonies were regarded as *M. ichthyoblabe* (including *M. flos-aquae*; Watanabe 1996). Photomicrographs of colonies were taken with an optical microscope (Scope. A1; Carl Zeiss Corporation, Oberkochen, Germany) and a digital camera (AxioCam ICc 3). The photomicrographs were analyzed for colony size, peripheral tightness, and surface cell arrangement using AxioVs40x64 V 4.9.1.0 (Carl Zeiss Corporation). The colony diameter ($D$, μm) was calculated as an equivalent circular diameter (Duan et al. 2018):

$$D = (4S/\pi)^{0.5} \tag{1}$$

where $S$ is the area of the colony ($\mu m^2$).

Colonies are flatter than balls, so it is more appropriate to calculate their volume as an ellipsoid rather than an ideal sphere. Therefore, the thickness was analyzed. According to Alcántara et al. (2018), thickness ($B$, μm) was measured as twice the microscope objective distance (10×), that is, $B = 2H$ (Fig. S1 in the Supporting Information). The colony volume ($V$, $\mu m^3$) was estimated as an ellipsoid:

$$V = 2BS/3 \tag{2}$$

The shape coefficient represented colony geometry (Ryabov et al. 2020):

$$\text{Shape coefficient} = D/B \tag{3}$$

Cell arrangement was analyzed as a spatial pattern of tightness. Each colony was added to 0.5 mL water and dispersed into single cells using a 100°C water-bath oscillator shaken at 120 rpm for 5 min (Joung et al. 2006). Then, the cell concentration in 0.5 mL water ($c_0$, $cells \cdot mL^{-1}$) was analyzed using a flow cytometer (BD Accuri C6 Plus, USA). Colony tightness was calculated using the following equation ($c$, $cells \cdot (100\ \mu m)^{-3}$):

$$c = \frac{0.5 c_0}{V \times 10^{-6}} \tag{4}$$

Peripheral tightness ($c_c$) and internal tightness ($c_r$) are the cell number per unit length in the circumferential and longitudinal direction of a colony, respectively ($cells \cdot 100\ \mu m^{-1}$; Fig. S2 in the Supporting Information). The cell arrangement on the surface of a colony was distinguishable at 100×

magnification. Therefore, peripheral tightness was directly measured under a microscope. Internal cells were indistinguishable, so internal tightness could not be measured directly. To obtain internal tightness and *CDR*, this study assumed that (i) the colony could be divided approximately into several regular square prisms, and the average value of all prisms represented the colony; (ii) cells were arranged as simple cubes in each prism; and (iii) tightness varied linearly between the top and bottom face of each prism following *CDR* >1, <1 and ≈1 (Fig. S2c). The peripheral tightness of prism $i$ was calculated using the following equations:

$$c^i_{sur.} = \frac{N^i_S\prime}{S_i\prime} \tag{5}$$

$$c^i_c = (c^i_{sur.})^{0.5} \tag{6}$$

wherein prism $i$, $c^i_{sur.}$ is the cell number per top face area (cells · (100 μm)$^{-2}$), $N^i_S\prime$ is the cell number in the top face, $S_i'$ is the top face area (μm$^2$); and $c^i_c$ is the peripheral tightness (cells · (100 μm)$^{-1}$).

The average value of $n$ uniformly distributed prisms was chosen to calculate the peripheral and internal tightness of the whole colony:

$$c_c = \frac{1}{n}\sum_{i=1}^{i=n} c^i_c \tag{7}$$

$$c_{sur.} = \frac{1}{n}\sum_{i=1}^{i=n} c^i_{sur.} \tag{8}$$

$$c_r = \frac{c}{c_{sur.}} \tag{9}$$

where $c_{sur.}$ is the cell number per surface area of a colony (cells · (100 μm)$^{-2}$).

Three structure types were proposed: homogeneous type (H-Type) if *CDR* ≈ 1, tighter-periphery type (T-Type) if *CDR* > 1, and looser-periphery type (L-Type) if *CDR* < 1 (Fig. S2c). The three types are intra-colony cells distributed homogeneously, tending to form pores, and gathering in the core of the colony.

*Field investigations.* To determine the structural variations under natural conditions, samples were collected from the middle of Meiliang Bay, Lake Taihu (120°10'28.80" E, 31°27'05.89" N) on January 15, March 17, April 18, May 10, May 24, and June 11, 2019, and September 7, 2018. Water samples (200 mL) were collected at depths of 0, 1.0, and 2.0 m (i.e., water surface, middle layer, and bottom, respectively). Algae samples were collected from the lake surface with a 64 μm phytoplankton net. All samples were stored at 4°C and transported to the laboratory for analysis.

Total nitrogen (TN), total phosphorus (TP), total dissolved nitrogen (DTN), and total dissolved phosphorus (DTP) were analyzed colorimetrically after digestion with $K_2S_2O_8$ + NaOH (Ebina et al. 1983). Ammonia nitrogen ($NH_4^+$-N) was detected by Nessler's reagent colorimetry (Zhu et al. 2018). Daily average air temperature and wind speed values for Wuxi city (~10 km from Meiliang Bay) were obtained from a network database (http://data.cma.cn/). Daily radiation was obtained from a network database (https://power.larc.nasa.gov/data-access-viewer/). The average meteorological data values from 2 to 4 weeks before sampling dates were used in the current study.

*Laboratory cultures.* A colonial strain of *Microcystis ichthyoblabe* from Meiliang Bay was used in this study (Duan et al. 2018), which was maintained in BG11 media at 25°C. All algae samples were precultured in a sterile incubator with "cool-white" fluorescent tubes (Saifu Corporation, China), which provided light of 45 μmol photons · m$^{-2}$ · s$^{-1}$ under a 12:12 h light:dark cycle. All utensils and media were autoclaved at 121°C for 30 min. Before culture tests, 20 mL samples during the exponential growth phase were used for inoculation, with an initial cell concentration of $5 \times 10^4$ cells · mL$^{-1}$. During the tests, samples were cultured in 500 mL Erlenmeyer flasks containing 200 mL BG11 media under the same conditions described above. One group of flasks was continuously oscillated with magnetic stirrers at 200 rpm. The other group was cultured under motionless conditions. The experiment was run for 15 d, and then the colonial structure and size were analyzed.

This study also compared the growth of this strain under different nutrient levels. The initial concentrations of TN and TP in BG11 media were adjusted (Table S1 in the Supporting Information). The strain was cultured in 250 mL Erlenmeyer flasks containing 150 mL of the four kinds of media under the same conditions described above. The initial cell concentration was $1 \times 10^4$ cells · mL$^{-1}$ and cells were cultured for 15 d. Cell concentration and colony diameter were analyzed every 3–4 d. Colony concentration and thickness were analyzed on the last day of cultivation.

*Statistical analysis.* Not all colonies, especially some small ones, may have their structure limited by colony size. The relationship between colony structure and size was analyzed using the interval maxima regression approach (IMR; Li et al. 2016). Each variable for thickness was divided into equal increments, resulting in 18 intervals. Then, the maximum values for cell arrangement in each interval were obtained, and linear fitting was applied to these maxima. Differences in colony size and structure from different groups were analyzed by one-way ANOVA after testing for homoscedasticity. All statistical analyses were conducted using R software (www.r-project.org/). Significance level was set at $P < 0.05$ in this study unless stated otherwise.

## RESULTS

*Characteristics of* Microcystis *colonies.* Colony samples were divided into four groups according to their origins. *Lab-s* and *Lab-t* were the colonies from motionless and oscillatory culture conditions, respectively, and *Microcystis aeruginosa* and *M. ichthyoblabe* colonies, respectively, collected from Lake Taihu. The diameter and thickness of *Lab-s* were 967–4042 μm and 395–895 μm, respectively, which were much higher than those of the other groups (Fig. 1a; ANOVA, $F_{3,147} = 65.06$, $P < 0.001$; and Fig. 1b, ANOVA, $F_{3,147} = 56.66$, $P < 0.001$). *Lab-t*, *M. aeruginosa*, and *M. ichthyoblabe* had similar thicknesses (approximately 50–400 μm), with an average and median value of 173–197 μm and 153–179 μm, respectively. However, colony size varied among *Lab-t*, *M. aeruginosa*, and *M. ichthyoblabe*. *Microcystis aeruginosa* had the largest diameter (1,633 μm) and *M. ichthyoblabe* had the smallest diameter (61 μm).

The structure among groups was also different (Fig. 1c). *Lab-s* had an irregular shape with a large superficial area and loose cell arrangement. *Lab-t* was strip-shaped and smooth-edged with a firm structure. The morphology of *Lab-t* was similar to that of *M. aeruginosa*. In addition, *M. aeruginosa* had the

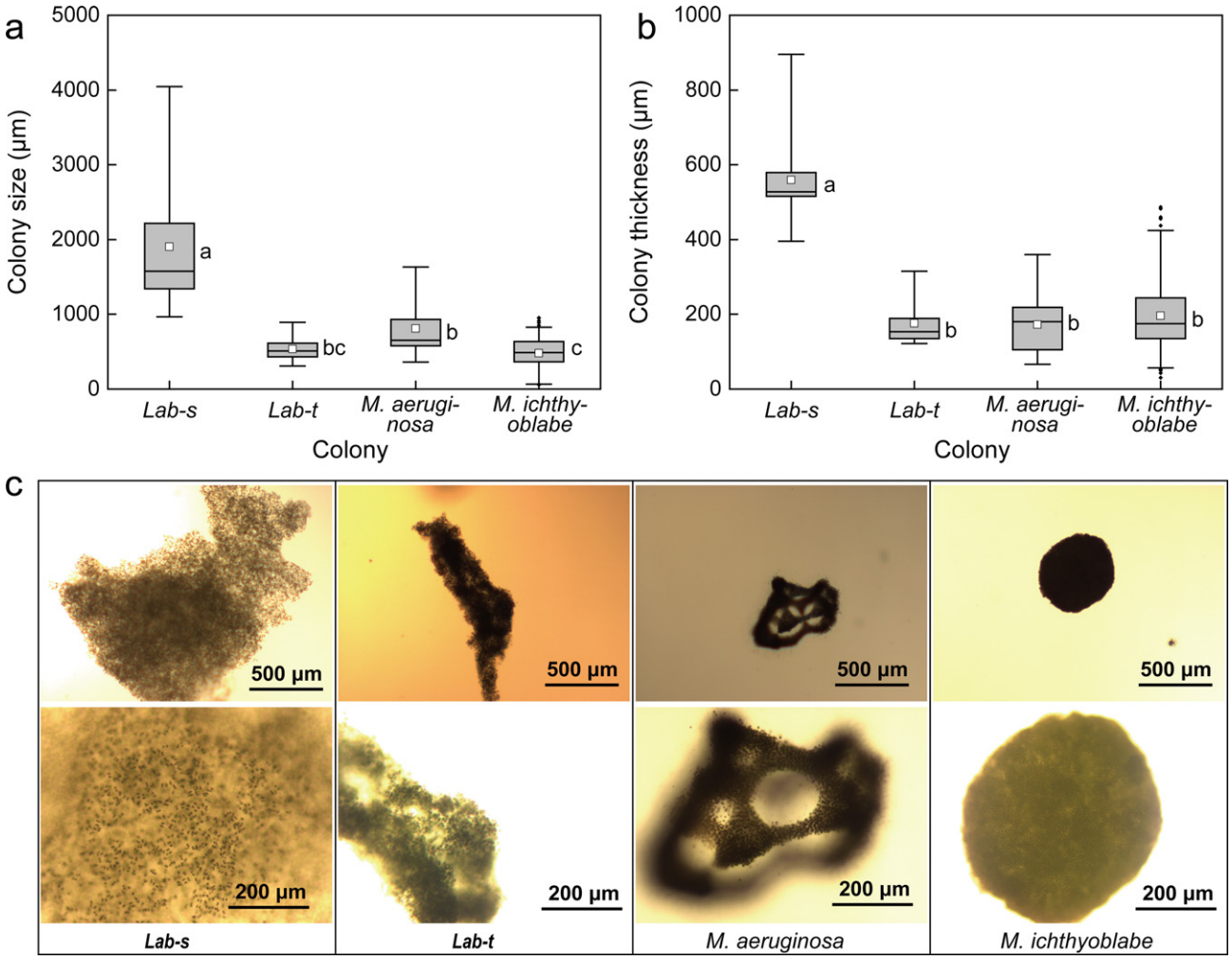


FIG. 1. Colony diameter (a), colony thickness (b), and photomicrographs (c) of colonies of *Lab-s*, *Lab-t*, *Microcystis aeruginosa*, and *M. ichthyoblabe*. Error bars of the 95th and 5th percentiles are shown together with values above or below these values, where appropriate. White square dots represent the mean values. The measurements of *Lab-s*, *Lab-t*, *M. aeruginosa*, and *M. ichthyoblabe* were 13, 15, 13, and 110, respectively. a, b, and c indicate significant ($P < 0.05$) differences among *Lab-s*, *Lab-t*, *M. aeruginosa*, and *M. ichthyoblabe* [Colour figure can be viewed at wileyonlinelibrary.com]

highest shape coefficient (~25), while *M. ichthyoblabe* had the lowest value (Fig. S3 in the Supporting Information; ANOVA, $F_{3,147} = 10.07$, $P < 0.001$). *Lab-s* was loosely arranged (122–697 cells · (100 μm)$^{-3}$), whereas the other groups were much tighter (337–4,761 cells · (100 μm)$^{-3}$; Fig. 2a; ANOVA, $F_{3,147} = 4.862$, $P < 0.01$). The results further showed that the tightness of *Lab-t* was similar to that of *M. aeruginosa* and *M. ichthyoblabe*. There was a distinguishable range of peripheral tightness ($c_c$) and internal tightness ($c_r$) in each group. The $c_c$ of *Lab-t* was higher than that of *Lab-s*. The *CDR*s of *Lab-s* and *M. ichthyoblabe* were obviously <1 and >1, respectively, while the *CDR* was approximately 1 in *Lab-t* and *M. aeruginosa* (ANOVA, $F_{3,147} = 6.677$, $P < 0.001$). Based on the definition of *CDR*, *Lab-t* and *M. aeruginosa* belonged to H-Type, *M. ichthyoblabe* belonged to T-Type, and *Lab-s* belonged to L-Type.

*Relationship between colony size and structure.* To investigate how the *Microcystis* colony increases in size and evolves in structure, this study analyzed the relationship between cell arrangement and thickness using the interval maxima regression approach. Figure 3 shows the trends of tightness, $c_c$, $c_r$, and *CDR*. There was a significantly negative correlation between the interval maxima tightness and thickness (IMR, $F_{1,12} = 23.12$, $R^2 = 0.63$, $P < 0.001$), that is, colonies grew in size at the cost of the structure being loose. The results were aligned with the theoretical optical limitation of Feng et al. (2019) (dotted line). The interval maxima values of $c_c$ and $c_r$ were also negatively correlated with thickness (Fig. 3 b, IMR, $F_{1,12} = 33.88$, $P < 0.001$; and Fig. 3c, IMR, $F_{1,12} = 10.68$, $P < 0.01$), except for the $c_c$ of *Lab-s*. In addition, the *CDR*s of *M. ichthyoblabe* and *Lab-s* were both positively correlated with thickness (IMR, $F_{1,108} = 5.265$, $P < 0.05$; and IMR, $F_{1,11} = 7.19$, $P < 0.05$), whereby the gap between peripheral and internal tightness increased significantly under

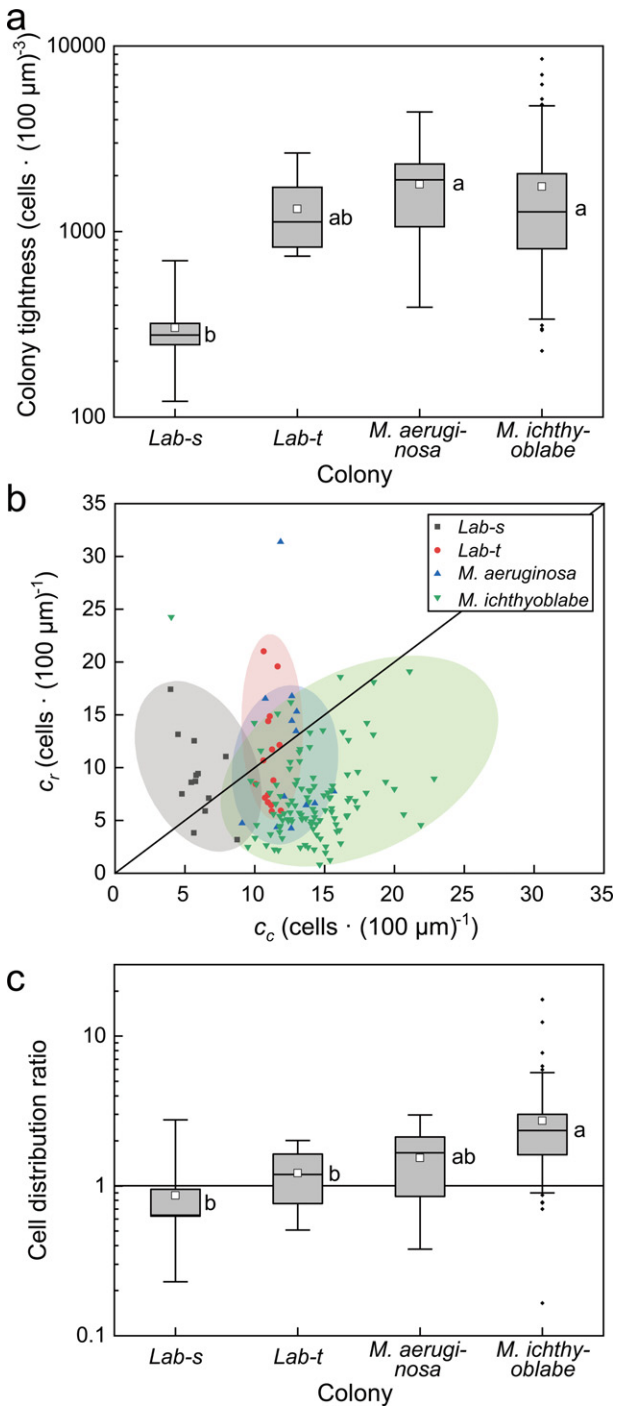


FIG. 2. Colony tightness (a), distribution of peripheral tightness ($c_c$) and internal tightness ($c_r$) (b), and cell distribution ratio (*CDR*) (c) of colonies of *Lab-s*, *Lab-t*, *Microcystis aeruginosa*, and *M. ichthyoblabe*. Error bars of the 95th and 5th percentiles are shown together with values above or below these values, where appropriate. White square dots represent the mean values. The measurements of *Lab-s*, *Lab-t*, *M. aeruginosa*, and *M. ichthyoblabe* were 13, 15, 13, and 110, respectively. a, b, and c indicate significant ($P < 0.05$) differences among *Lab-s*, *Lab-t*, *M. aeruginosa*, and *M. ichthyoblabe* [Colour figure can be viewed at wile yonlinelibrary.com]

elevated colony size. However, the *CDR*s of *M. aeruginosa* and *Lab-t* were not significantly correlated with thickness (IMR, $F_{1,11} = 1$, $P = 0.3387$; and IMR, $F_{1,13} = 1.216$, $P = 0.2902$). There was a higher quality of correlation and significance in IMR than when all the samples were used (Fig. 3b, OR, $F_{1,149} = 85.24$, $R^2 = 0.360$, $P < 0.001$; Fig. 3c, OR, $F_{1,149} = 2.105$, $R^2 = 0.007$, $P = 0.149$), which verified the advantage of the IMR method.

*Effects of turbulence shear and nutrient limits on colony size and structure.* Figure 1 and Figure S3 show that turbulence changed the shape of colonies as described above. This study further confirmed that turbulence caused the inhomogeneity of the cell arrangement (Fig. 2). Colonies in Level 1 had the largest diameter ($D_{50} > 1{,}000$ μm), where colonies also increased the fastest in size (Fig. 4a; ANOVA, $F_{3,4} = 28.54$, $P < 0.01$). Surprisingly, colonies with sufficient nutrient supply grew the most slowly. The top cell concentration (~$290 \times 10^4$ cells · mL$^{-1}$) and top colony concentration (~1,400 colonies · mL$^{-1}$) appeared in Level 2 rather than in Level 1. The cell concentration decreased from Level 2 to Level 4, but was still clearly higher than that of Level 1 (ANOVA, $F_{3,4} = 35.5$, $P < 0.01$). In addition, colonies in Level 1 and Level 2 were large and loose; while the others were much smaller and compact. Colonies in Levels 2–4 were similar to the wild-type colonies, especially the holes in colonies with $D_{50}$ of ~190–250 μm.

*Structural variations in colonies in Lake Taihu.* The monthly average air temperature, wind speed, solar radiation, and water quality parameters of Meiliang Bay are listed in Figure S4 in the Supporting Information. Water quality parameters include TN, TP, $NH_4^+$-N, DTN, and DTP. The average air temperature was 5°C in January, which rose to 8°C in March and 23°C in May. Wind speed ranged from 1.54 to 2.16 m · s$^{-1}$. Solar radiation was 7.0 to 7.5 kW · hm$^{-2}$ · d$^{-1}$ from January to February, and rose to 9 kW · hm$^{-2}$ · d$^{-1}$ in May. TN, TP, DTN, DTP, and $NH_4^+$-N were 1.61–4.26 mg · L$^{-1}$, 0.04–-0.68 mg · L$^{-1}$, 0.32–1.63 mg · L$^{-1}$, 0.01–-0.13 mg · L$^{-1}$, and 0.03–0.51 mg · L$^{-1}$, respectively. DTN and DTP decreased from January to June.

*Microcystis ichthyoblabe* was the dominant morphospecies from January to June, and was chosen here to analyze seasonal variations. Figure 5 shows the diversity in structure and size. The colony diameter continued to rise; however, the average and median value of thickness slightly declined after its peak in April. Surprisingly, the 95th percentile of thickness continued to increase monthly, especially from March to April. Tightness decreased considerably from March to April, and increased after April (ANOVA, $F_{4,85} = 17.22$, $P < 0.001$). Under a light source, the light permeability of colonies exhibited obvious seasonal variations. Compared with January, colonies from April to June were relatively loose and allowed more light to pass through. These colonies also had higher peripheral tightness and lower internal tightness, except for $c_c$ of colonies in April. Additionally, the *CDR* from March to June was

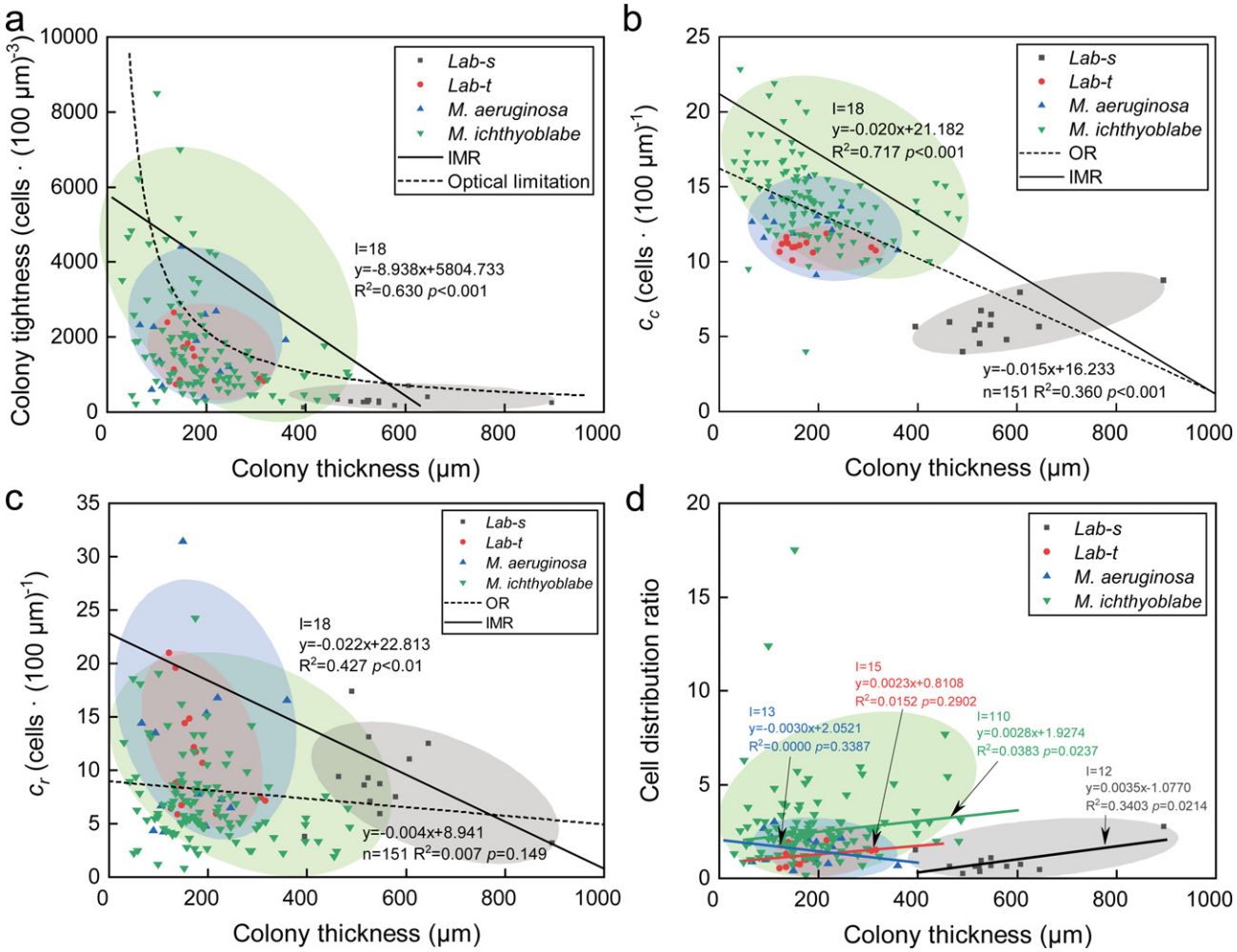


FIG. 3. Relationships between colony thickness and colony tightness (a), peripheral tightness ($c_c$) (b), internal tightness ($c_r$) (c), and cell distribution ratio (d). OR and IMR present the linear regression of all samples and the interval maxima, respectively. The optical limitation represents the limit of light on the maximum colony thickness ($B_{Max}$) and tightness ($c$) according to the following equation: $B_{Max} = 4.3 \times 10^5 \cdot c^{-1}$ (Feng et al. 2019). The number of IMR intervals is 18 [Colour figure can be viewed at wileyonlinelibrary.com]

higher than that in January. Mean *CDR* values declined from March to June while the median value was generally unchanged.

## DISCUSSION

This study investigated the size and structure of *Microcystis* colonies as well as the mechanism of structural variations. A significant negative correlation was identified between the colonial structure and size (Fig. 3). Such a relationship indicates the constraints of size on colonial structure and the related strategies of *Microcystis* to bypass this limitation. The results show that the colonial structure and size varied among different origins. Colonies of *Lab-s* were much larger and thicker than wild colonies while they were looser in structure. Such atypical colonies in the laboratory may be attributed to (i) continuous cell division generating a large number of cells under sufficient nutrient supply (Duan et al. 2018) and (ii) synthesis of large amounts of extracellular polysaccharides to fill in the space among cells (Tan et al. 2020). Instead, *Microcystis* reappeared with the morphology of the wild-type colonies under turbulent shear or nutrient limits (Fig. 4).

The results show that turbulence and nutrient limits are important influencing factors for maintaining typical wild morphologies. Nutrient limits and turbulent shear likely affect colony geometry and cell arrangement. Low nutrient concentrations resulted in intra-colony pores, which also contributed to the decline in size. Additionally, it is well known that turbulence has a shear effect on particles (Guasto et al. 2012). In our present study, turbulent shear stretched and compacted colonies: *Lab-s* was irregular and loose, whereas *Lab-t* was rod-shaped and tight. The upward trends in the 5$^{th}$ percentile of peripheral tightness from January to June might be due to the upward trends in wind-induced

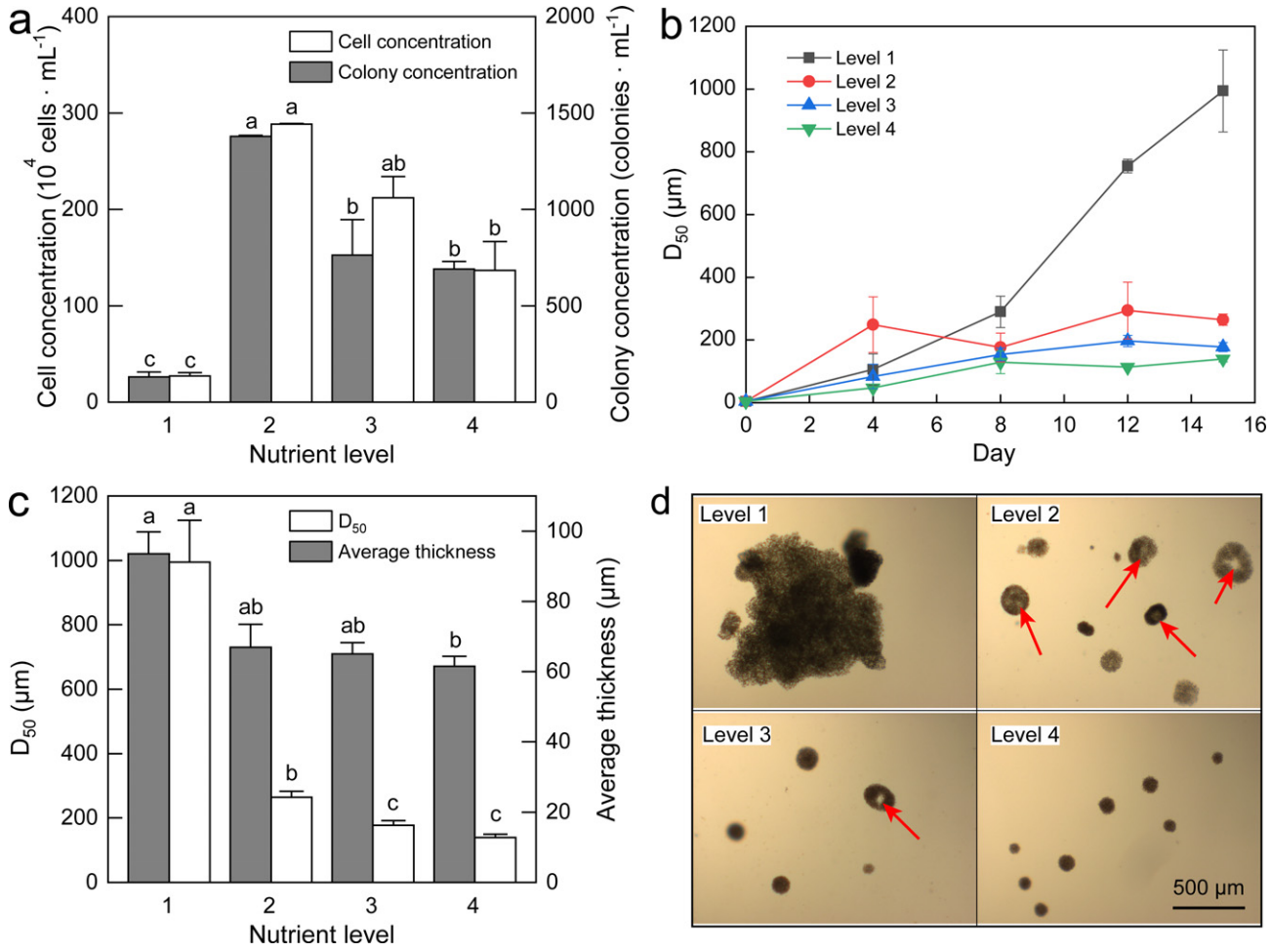


FIG. 4. Relationships between initial nutrient levels and final concentrations of cells or colonies (a), $D_{50}$ change (b), and final $D_{50}$ and thickness (c). a, b, and c indicate significant ($P < 0.05$) differences among nutrient levels (Mean ± SD, $n = 2$). Photomicrograph of colonies under different nutrient levels (d). Arrows indicate holes in colonies [Colour figure can be viewed at wileyonlinelibrary.com]

turbulent mixing. Moisander et al. (2002) analyzed the effect of small-scale turbulence on the physiological activities and morphology of cyanobacteria and identified a shear effect. In addition, fierce shear can destroy colonies (O'Brien et al. 2004, Li et al. 2018). Therefore, turbulent shear and insufficient nutrients might be underlying prerequisites for culturing wild-type colonies. What selection pressures favor oblate or rod-shaped colonies? What environmental niche do these colonies occupy? Is there a link between loose cell arrangement (or perforated shape) and bloom formation? Answering these questions may contribute to a better understanding of the complex ecological constraints on the growth of *Microcystis*.

One of the growth traits of *Microcystis* is the decrease in colonial tightness under larger colony sizes. Large and tight structures adversely affect the allocation of resources, such as light (Feng et al. 2019), carbon (Paerl 1983), and dissolved oxygen (Fang et al. 2018). Therefore, variations in colonial structure may be a result of the constraints from colony size and cellular metabolism, which is apparent under environmental stresses such as nutritional limits or shear. Further evidence implies holes in the colonies, since *M. ichthyoblabe* diverged into *M. aeruginosa* when the internal cells were under stagnation or withered (Reynolds et al. 1981). There were also similar holes in the colonies under nutrient-limited cultures and natural conditions. Therefore, $CDR > 1$ may be a result of the relatively low growth rate in the core of colonies. As soon as internal cells stop proliferating and *CDR* becomes approximately infinite, colonies may form holes. Similar phenomena also exist in other species, for example, *Phaeocystis globose*, *Sphaerocavum Brasiliense*, *Volvox*, and *Sorastrum* (Marchant 1974, Van Rijssel et al. 1997, Hans and Kam 2002, de P Azevedo and Sant' Anna 2003, Yamashita and Nozaki 2019). Another trait is that most colonies are oblate or perforated (i.e., diameter > thickness). Culture tests indicate that colonies under nutrient constraints prefer to develop dimensions along the direction of the colony's long axis, which would improve their

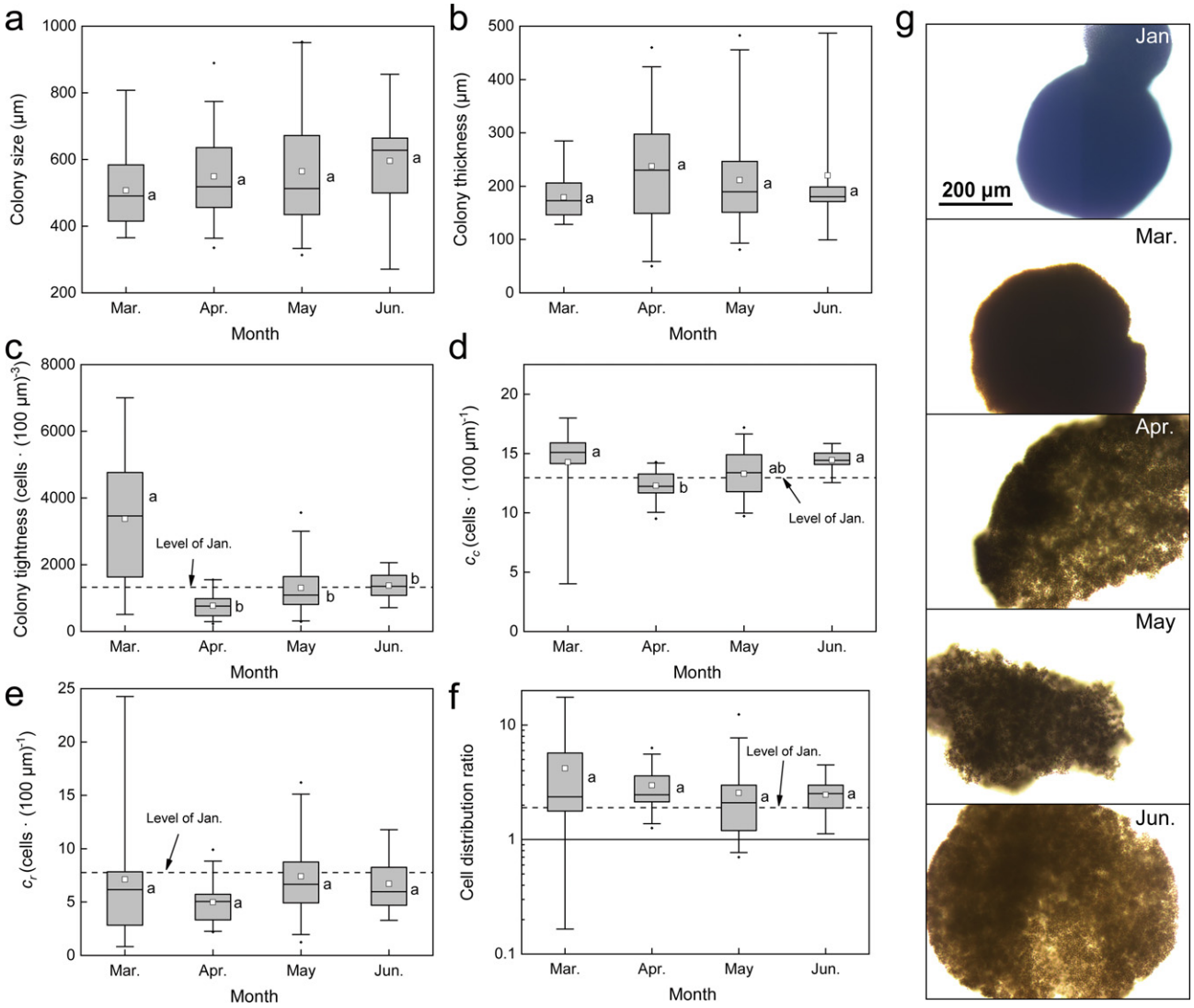


FIG. 5. Monthly variations in *Microcystis ichthyoblabe* colony diameter (a), colony thickness (b), colony tightness (c), peripheral tightness (d), internal tightness (e), and cell distribution ratio (f). The measurements of samples of March, April, May, and June are 11, 26, 38, and 13, respectively. a and b indicate significant differences ($P < 0.05$) among March, April, May, and June. Error bars of 95th and 5th percentile are shown together with values above or below these values, where appropriate. White square dots represent the mean values. A microphotograph of *M. ichthyoblabe* colonies from January to June 2019 (g) [Colour figure can be viewed at wileyonlinelibrary.com]

specific surface area. The variations in colonial structure and size here are also consistent with the tradeoff law of phytoplankton proposed by Naselli-Flores et al. (2020).

This study supposes that the above two traits promote structural variations and help large colonies to maintain normal metabolism. Loose or porous colonial structures can relieve the crowd effect of cells and resource blocks, and therefore, break through the limit of growth. The seasonal succession of different morphologies might be a type of adaptation effort. These traits indicate at least three probable transition pathways of variation (Fig. 6). Generally, tightness decreases with larger colony sizes. Under natural conditions or low nutrient levels, size constraint is noticeable in thick colonies, which results in a relatively low growth rate of internal cells, increase in *CDR* and, and finally, the formation of holes (Transition route 1). Colonies in undisturbed cultures have a loose structure; thus, the growth rate between peripheral and internal cells is similar, and therefore, $CDR < 1$ (Transition route 2-1). Turbulent shear increases *CDR*, stretches colonies, and decreases colony size (Transition route 2-2).

Our findings are also novel for understanding the ecological strategies in the seasonal patterns of *Microcystis*. The *Microcystis ichthyoblabe* colony structure became loose and formed pores due to the constraints from the colony size. Our results indicate that loose *M. wesenbergii* and perforated *M. aeruginosa* commonly grow in much larger colonies and dominate blooms after spring because their

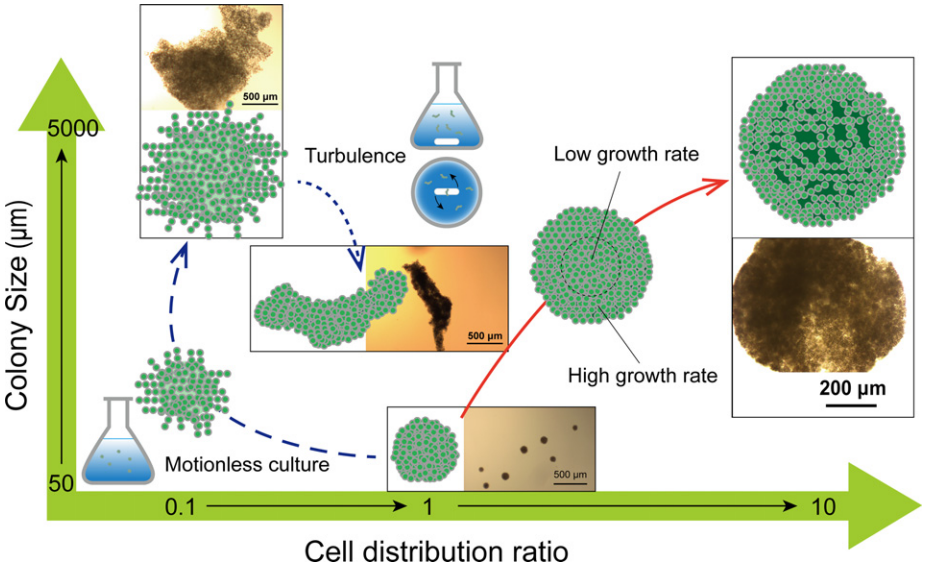


FIG. 6. Transition pathways of colony-structural changes. Transition route 1 (arrow with solid line): from homogeneous type (H-Type) to tighter-periphery type (T-Type). Transition route 2-1 (long dashed arrow): from H-Type to looser-periphery type (L-Type) under motionless laboratory culture. Transition route 2-2 (short dotted arrow): L-Type converts to H-Type due to turbulent shear [Colour figure can be viewed at wileyonlinelibrary.com]

morphologies are less limited by colony size. Colonies elevate size as compensation for becoming loose or porous. A recent review showed that an increase in colony size caused a significant increase in bloom formation (Xiao et al. 2018). Large-sized *M. wesenbergii* and *M. aeruginosa* are more suitable than *M. ichthyoblabe* for competing over other phytoplankton in the warm summer and autumn. Therefore, structural variations are beneficial strategies for *Microcystis* forming blooms.

## CONCLUSIONS

In summary, this study evaluated the characteristics of *Microcystis* colonies and is the first to report three structural types: H-type, T-Type, and L-Type. Based on the results obtained, this study concludes that colony size affects colonial structure. More specifically, colony size affects colony structure, probably by limiting the growth of intra-colony cells. In addition, environmental factors may affect variations in the colonial structure. Based on these results, this study proposes three transition routes for structural variations in *Microcystis* colonies. Our results highlight that cells arrange loosely in large colonies to maintain growth. Therefore, structural variations may be survival strategies for breaking through the growth limit of colony size, resulting in higher colony size and ecological benefits for *Microcystis*.

The authors gratefully acknowledge the financial support received from the Science and Technology Project of Jiangsu Province (BE2018737), the National Science and Technology Major Project of the Ministry of Science and Technology of China (2017ZX07603-003-04), and the World-Class Universities (Disciplines) and Characteristic Development Guidance Funds for the Central Universities.

Alcántara, I., Piccini, C., Segura, A. M., Deus, S., González, C., Martínez de la Escalera, G. & Kruk, C. 2018. Improved biovolume estimation of *Microcystis aeruginosa* colonies: a statistical approach. *J. Microbiol. Methods* 151:20–27.

Aparicio Medrano, E., van de Wiel, B. J. H., Uittenbogaard, R. E., Dionisio Pires, L. M. & Clercx, H. J. H. 2016. Simulations of the diurnal migration of *Microcystis aeruginosa* based on a scaling model for physical-biological interactions. *Ecol. Modell.* 337:200–10.

de P Azevedo, M. T. & Sant' Anna, C. L. 2003. *Sphaerocavum*, a new genus of planktic cyanobacteria from continental water bodies in Brazil. *Algol. Stud.* 109:79–92.

Duan, Z., Tan, X., Parajuli, K., Upadhyay, S., Zhang, D., Shu, X. & Liu, Q. 2018. Colony formation in two *Microcystis* morphotypes: effects of temperature and nutrient availability. *Harmful Algae* 72:14–24.

Ebina, J., Tsutsui, T. & Shirai, T. 1983. Simultaneous determination of total nitrogen and total phosphorus in water using peroxodisulfate oxidation. *Water Res.* 17:1721–26.

Fang, F., Gao, Y., Gan, L., He, X. & Yang, L. 2018. Effects of different initial pH and irradiance levels on cyanobacterial colonies from Lake Taihu. *China. J. Appl. Phycol.* 30:1777–93.

Feng, G., Zhu, W., Hu, S., Xue, Z., Wang, R. & Chen, H. 2019. Attenuation of light influences the size of *Microcystis* colonies. *Harmful Algae* 89:101667.

Gan, N., Xiao, Y., Zhu, L., Wu, Z., Liu, J., Hu, C. & Song, L. 2012. The role of microcystins in maintaining colonies of bloom-forming *Microcystis* spp. *Environ. Microbiol.* 14:730–42.

Guasto, J. S., Rusconi, R. & Stocker, R. 2012. Fluid mechanics of planktonic microorganisms. *Annu. Rev. Fluid Mech.* 44:373–400.

Hans, H. J. & Kam, W. T. 2002. Effects of protozoan grazing on colony formation in *Phaeocystis globosa* (Prymnesiophyceae) and the potential costs and benefits. *Aquat. Microb. Ecol.* 27:261–73.

Jochimsen, E. M., Carmichael, W. W., An, J., Cardo, D. M., Cookson, S. T., Holmes, C. E. M., Antunes, M. B. et al. 1998. Liver failure and death after exposure to microcystins at a hemodialysis center in Brazil. *N. Engl. J. Med.* 338:873–78.

Joung, S. H., Kim, C. J., Ahn, C. Y., Jang, K. Y., Boo, S. M. & Oh, H. M. 2006. Simple method for a cell count of the colonial Cyanobacterium, *Microcystis* sp. *J. Microbiol.* 44:562.

Kromkamp, J. & Walsby, A. E. 1990. A computer model of buoyancy and vertical migration in cyanobacteria. *J. Plankton Res.* 12:161–83.

Li, M., Peng, Q. & Xiao, M. 2016. Using interval maxima regression (IMR) to determine environmental optima controlling *Microcystis* spp. growth in Lake Taihu. *Environ. Sci. Pollut. Res.* 23:1–11.

Li, M., Xiao, M., Zhang, P. & Hamilton, D. P. 2018. Morphospecies-dependent disaggregation of colonies of the cyanobacterium *Microcystis* under high turbulent mixing. *Water Res.* 141:340–48.

Li, M., Zhu, W., Gao, L., Huang, J. & Li, L. 2013a. Seasonal variations of morphospecies composition and colony size of *Microcystis* in a shallow hypertrophic lake (Lake Taihu, China). *Fresenius Environ. Bull.* 22:3474–83.

Li, M., Zhu, W., Gao, L. & Lu, L. 2013b. Changes in extracellular polysaccharide content and morphology of *Microcystis aeruginosa* at different specific growth rates. *J. Appl. Phycol.* 25:1023–30.

Marchant, H. J. 1974. Mitosis, cytokinesis, and colony formation in the green alga *Sorastrum*. *J. Phycol.* 10:107–20.

Moisander, P., Hench, J. L., Kononen, K. & Paerl, H. W. 2002. Small-scale shear effects on heterocystous cyanobacteria. *Limnol. Oceanogr.* 47:108–19.

Naselli-Flores, L., Zohary, T. & Padisák, J. 2020. Life in suspension and its impact on phytoplankton morphology: an homage to Colin S. Reynolds. *Hydrobiologia*, https://doi.org/10.1007/s10750-020-04217-x.

Nielsen, S. L., Enriquez, S., Duarte, C. & Sand-Jensen, K. 1996. Scaling maximum growth rates across photosynthetic organisms. *Funct. Ecol.* 10:167–75.

O'Brien, K. R., Meyer, D. L., Waite, A. M., Ivey, G. N. & Hamilton, D. P. 2004. Disaggregation of *Microcystis aeruginosa* colonies under turbulent mixing: laboratory experiments in a grid-stirred tank. *Hydrobiologia* 519:143–52.

Paerl, H. W. 1983. Partitioning of $CO_2$ Fixation in the colonial cyanobacterium *Microcystis aeruginosa*: Mechanism promoting formation of surface scums. *Appl. Environ. Microbiol.* 46:252–59.

Paerl, H. W. & Otten, T. G. 2013. Harmful cyanobacterial blooms: Causes, consequences, and controls. *Microb. Ecol.* 65:995–1010.

Qin, B., Paerl, H. W., Brookes, J. D., Liu, J., Jeppesen, E., Zhu, G., Zhang, Y., Xu, H., Shi, K. & Deng, J. 2019. Why Lake Taihu continues to be plagued with cyanobacterial blooms through 10 years (2007–2017) efforts. *Sci. Bull.* 64:354–56.

Reynolds, C. S., Jaworski, G. H. M., Cmiech, H. A. & Leedale, G. F. 1981. On the annual cycle of the blue-green alga *Microcystis Aeruginosa* Kütz. Emend. Elenkin. *Philos. Trans. R. Soc. London* 293:419–77.

Ryabov, A., Kerimoglu, O., Litchman, E., Olenina, I., Roselli, L., Basset, A., Stanca, E. & Blasius, B. 2020. Shape matters: cell geometry determines phytoplankton diversity. bioRxiv 2020. 02.06.937219.

Shan, K., Song, L., Chen, W., Li, L., Liu, L., Wu, Y., Jia, Y., Zhou, Q. & Peng, L. 2019. Analysis of environmental drivers influencing interspecific variations and associations among bloom-forming cyanobacteria in large, shallow eutrophic lakes. *Harmful Algae* 84:84–94.

Shen, H., Niu, Y., Xie, P., Tao, M. I. N. & Yang, X. I. 2011. Morphological and physiological changes in *Microcystis aeruginosa* as a result of interactions with heterotrophic bacteria. *Freshwater Biol.* 56:1065–80.

Su, M., Andersen, T., Burch, M., Jia, Z., An, W., Yu, J. & Yang, M. 2019. Succession and interaction of surface and subsurface cyanobacterial blooms in oligotrophic/mesotrophic reservoirs: a case study in Miyun Reservoir. *Sci. Total Environ.* 649:1553–62.

Tan, X., Shu, X., Duan, Z. & Parajuli, K. 2020. Two types of bound extracellular polysaccharides and their roles in shaping the size and tightness of *Microcystis* colonies. *J. Appl. Phycol.* 32:255–262.

Van Rijssel, M., Hamm, C. E. & Gieskes, W. W. C. 1997. *Phaeocystis globosa* (Prymnesiophyceae) colonies: hollow structures built with small amounts of polysaccharides. *Eur. J. Phycol.* 32:185–92.

Verspagen, J. M. H., Van de Waal, D. B., Finke, J. F., Visser, P. M. & Huisman, J. 2014. Contrasting effects of rising $CO_2$ on primary production and ecological stoichiometry at different nutrient levels. *Ecol. Lett.* 17:951–60.

Watanabe, M. 1996. Isolation, cultivation and classification of bloom-forming *Microcystis* in Japan. *Toxic Microcystis* 2:13–34.

Wilson, A. E., Kaul, R. B. & Sarnelle, O. 2010. Growth rate consequences of coloniality in a harmful phytoplankter. *PLoS ONE* 5:e8679.

Wu, X. & Kong, F. 2009. Effects of light and wind speed on the vertical distribution of *Microcystis aeruginosa* colonies of different sizes during a summer bloom. *Int. Rev. Hydrobiol.* 94:258–66.

Wu, X., Wu, H., Wang, S., Wang, Y., Zhang, R., Hu, X. & Ye, J. 2018. Effect of propionamide on the growth of *Microcystis flos-aquae* colonies and the underlying physiological mechanisms. *Sci. Total Environ.* 630:526–35.

Xiao, M., Hamilton, D. P., O'Brien, K. R., Adams, M. P., Willis, A. & Burford, M. A. 2020. Are laboratory growth rate experiments relevant to explaining bloom-forming cyanobacteria distributions at global scale? *Harmful Algae* 92:101732.

Xiao, M., Li, M. & Reynolds, C. S. 2018. Colony formation in the cyanobacterium *Microcystis*. *Biol. Rev.* 93:1399–420.

Yamamoto, Y., Shiah, F. K. & Chen, Y. L. 2011. Importance of large colony formation in bloom-forming cyanobacteria to dominate in eutrophic ponds. *Ann. Limnol. Int. J. Lim.* 47:167–73.

Yamashita, S. & Nozaki, H. 2019. Embryogenesis of flattened colonies implies the innovation required for the evolution of spheroidal colonies in volvocine green algae. *BMC Evol. Biol.* 19:120.

Yang, Z., Kong, F., Yang, Z., Zhang, M., Yu, Y. & Qian, S. 2009. Benefits and costs of the grazer-induced colony formation in *Microcystis aeruginosa*. *Ann. Limnol. Int. J. Lim.* 45:203–8.

Zhu, W., Zhou, X., Chen, H. & Li, M. 2018. Sequence of *Microcystis* colony formation during recruitment under natural conditions. *Hydrobiologia* 823:39–48.

## Supporting Information

Additional Supporting Information may be found in the online version of this article at the publisher's web site:

**Fig. S1.** Photomicrograph of *Microcystis* colonies. Each colony is placed on a slide beneath the objective lens (a, b). Thickness ($B$) is defined as twice the microscope objective distance ($H$), which is measured by adjusting the lens from the first to the last visible cell (c)

**Fig. S2.** A schematic model for analyzing peripheral tightness ($c_c$), internal tightness ($c_r$) and cell distribution ratio ($CDR$). The colony is divided into regular square prisms, and this study assumes that cells (green circles) are arranged as a simple cube in each prism (a). Distinguishable cell arrangements and sampling areas on the surface of colonies (b). Tightness is assumed to vary linearly in each prism following three modes

(*CDR* <1, >1, and ≈1) (c). Other abbreviations are described in the text

**Fig. S3.** Shape coefficients of colonies of *Lab-s*, *Lab-t*, *Microcystis aeruginosa*, and *M. ichthyoblabe*. Error bars of the 95th and 5th percentiles are shown together with values above or below these values, where appropriate. White square dots represent the mean values. The measurements of *Lab-s*, *Lab-t*, *M. aeruginosa*, and *M. ichthyoblabe* were 13, 15, 13, and 110, respectively. a and b indicate significant ($P < 0.05$) differences among *Lab-s*, *Lab-t*, *M. aeruginosa*, and *M. ichthyoblabe*

**Fig. S4.** The meteorological factors and water quality in Meiliang Bay from January to June 2019. Meteorological factors include temperature (a), wind speed (b), and solar radiation (c). Water quality parameters include total nitrogen (TN) (d), total phosphorus (TP) (e), ammonia nitrogen ($NH_4^+$-N) (f), total dissolved nitrogen (DTN) (g), and total dissolved phosphorus (DTP) (h). Data of water quality is represented as Mean ± SD ($n = 3$)

**Table S1.** Initial concentrations of total nitrogen (TN) and total phosphorus (TP) in Levels 1, 2, 3, and 4, respectively.